Growth of epitaxial bcc Co(001) electrodes for magnetoresistive devices

H. Wieldraaijer,* J. T. Kohlhepp, P. LeClair, K. Ha, and W. J. M. de Jonge
Eindhoven University of Technology, Department of Applied Physics, Center for Nanomaterials (CNM) and COBRA Research Institute, P.O. Box 513, 5600 MB Eindhoven, The Netherlands
(Received 7 February 2003; published 25 June 2003)

The applicability of the strain-induced bcc phase of Co in magnetoresistive devices was studied. Ultrathin bcc Co(001) films and the influence of the additional layers needed for magnetoresistive devices were examined by means of ^{59}Co nuclear magnetic resonance (NMR). NMR is shown to be a discriminating technique for determining the presence of structurally and magnetically pure bcc Co. The maximum stability for uncovered and Fe-covered layers grown on Fe(001)/GaAs(001) and Fe(001)/Ge(001) seed layers is found to be about 2 nm. Growth of an Al_2O_3 top layer preserves the bcc phase, in contrast to a Cu film which causes a transformation of the bcc structure to the fcc or the hcp phase. The bcc-preserving effects of Al_2O_3 imply the possibility to fabricate magnetic tunnel junctions with bcc Co(001) bottom electrodes. Although bcc Co is a force-induced structure, thin layers are shown to be stable over a few years when Al_2O_3 has been grown on top. Junction structures using bcc Co(001) bottom electrodes were grown and characterized.

DOI: 10.1103/PhysRevB.67.224430 PACS number(s): 68.55.Jk, 75.70.Ak, 73.40.Gk, 85.70.Kh

I. INTRODUCTION

Tunneling processes in magnetic tunnel junctions[1] (MTJ's) are largely determined by the electronic structure of the active layers. A theoretical description of spin-polarized tunneling, based on the electronic structure, is quite feasible for idealized structures and fully epitaxial layers with sharp interfaces.[2–4] A complete description for realistic junction structures is however extremely difficult. The largest problem is the lack of crystalline order of the Al_2O_3 barrier commonly used in MTJ's, which is very difficult to model theoretically. In addition, the roughness and slight intermixing at the interfaces, and the nonepitaxy of, at least, the upper electrode which is grown on the Al_2O_3 barrier also pose enormous problems. A way to circumvent the source of these problems is the growth of semiepitaxial junctions, where the lower electrode is grown in a single-crystalline structure. The barrier and the upper electrode are still amorphous and polycrystalline, respectively. The well-defined structure of the bottom electrode offers the opportunity to investigate the effect of a specific physical and electronic structure on the tunnel properties. By varying the structure of the bottom electrode in a controlled way this effect can be separated from the general properties of the junction. In this way, an understanding of the properties influencing tunnel junctions can be obtained without the need for a full theoretical description. An advantage of this method with respect to the use of fully epitaxial junctions is that in semiepitaxial junctions the structure of the bottom electrode can be varied without influencing the rest of the junction stack. The barrier and the top electrode will still have the same physical and electronic properties. This procedure has been used by Yuasa *et al.*, who established a dependence of the tunneling spin polarization on the crystallographic orientation for epitaxial bcc Fe bottom electrodes[5] and demonstrated resonant tunneling in MTJ's with epitaxial Cu-dusted fcc Co bottom electrodes.[6] Recently, LeClair *et al.*[7] observed clear band-structure effects in MTJ's with Co electrodes by using bottom electrodes consisting of either Co in a fcc-(111) phase or of Co in a polycrystalline mixed fcc/hcp phase. These band-structure effects could be explained qualitatively and, in part, quantitatively by a model based on elastic tunneling using the calculated band structures for the different Co phases.

Co is an ideal material for investigating the influence of the physical and electronic structure because it can be stabilized in different crystal phases. The hcp structure is the stable bulk phase at room temperature and the fcc structure is very easy to obtain in thin-film growth by stabilization on appropriate substrates or at elevated temperatures.[8] For fcc Co, the substrate does not even need to have an epitaxial relationship with Co. On certain substrates, Co will grow at room temperature in a polycrystalline phase which will order itself into fcc above thicknesses of a few nanometers.[9] Under specific conditions, thin Co films can also be stabilized in the bcc phase. For Co, this phase is strain induced by epitaxy with the substrate. The first report of bcc Co, made by Prinz,[10] used growth on GaAs(110). Later, bcc Co was stabilized in between Fe layers and Cr layers,[11] in between Au layers,[12] and on some alloy substrates such as TiAl[13] and $CoSi_2/Si(001)$.[14] In the following section, we will give a short overview of the reports on bcc Co in the literature.

For using bcc Co in device structures, growth of another layer on top of the bcc Co, e.g., Al_2O_3 or Cu, is inevitable. The effect of these overlayers on the underlying bcc Co is not known. For some materials, a recrystallization of the top part of the bcc Co into a different crystal phase may occur. This recrystallization may disturb a large part of the bcc Co, since typical stability limits are below 20 ML (monolayer). To our knowledge, no studies have been reported on the influence of additional layers on the bcc structure, apart from layers such as Fe that are already known as bcc-inducing substrates. Device structures using Cu layers on top of bcc Co were reported,[15] however without verification of the stability of the bcc Co.

In this study, we investigate the influence of different top layers on the stability and structure of ultrathin bcc Co layers and show that it is indeed possible to grow these layers in such a way that they can be used in MTJ's. This result pro-

vides a new Co phase to be used in these devices, which allows for a more complete investigation of the influence of crystal structure on tunneling properties. We also show that Cu top layers, which are used in other device structures, do induce a structural change in the Co layer. The paper is organized as follows. In the following section, we will first briefly review the growth of bcc Co as reported in the literature. In Sec. III, we will present the details of our sample preparation and analysis. The characterization of the physical and magnetic structure of the uncovered layers will be given in Sec. IV. In Sec. V the results are presented, which are obtained by ^{59}Co nuclear magnetic resonance (NMR) on Co layers with different layers grown on top. In Sec. VI, the results of magnetoresistance measurements on a junction structure with a bcc Co(001) bottom electrode are reported, followed by a discussion of the results on the stability of bcc Co and the important conclusions of our study.

II. STABILITY AND ANALYSIS OF BCC CO

A large number of studies have been published on the growth of bcc Co. Very different growth and characterization techniques were employed, and sometimes conflicting results were obtained.

Although early calculations predicted bcc Co to be a metastable phase, more recent papers showed that the bcc phase is unstable against volume-conserving tetragonal distortions.[16–18] The true metastable phase is a body-centered tetragonal (bct) phase, with a c/a ratio of 0.92, where c is the lattice constant in the growth direction and a is the lattice constant in the plane perpendicular to the growth direction. The energy barrier stabilizing this phase against tetragonal deformation into the fcc phase, which is obtained when $c/a = 1.41$, is however extremely low (0.7 meV). This makes it almost impossible to stabilize thick, pure bct Co films. In practice, all pure bcc or bct Co layers can only be stabilized by epitaxy on lattice matched substrates that put a constraint on the in-plane lattice parameter for a limited thickness. We will use the expression bcc Co in this paper even when the layer is strained ($c/a \neq 1$), because both bcc and bct Co are, in practice, strain-induced phases and all grown layers show some strain.

The fact that bcc Co is strain induced has major consequences on its properties and growth. The substrate and the exact growth conditions have a strong influence on the stability of the layers and the resulting strain in them. This influence caused some controversy on the maximum stability of bcc Co. Papers by Prinz and co-workers[10,19,20] and by Bland *et al.*[21] report bcc Co with thicknesses up to 35.7 nm and 14.5 nm by growth on GaAs(110) and (001), respectively. However, many other groups show stability limits in the range of 10–20 ML (i.e. less than 3 nm) for various substrates (including GaAs) and crystal orientations.[11,12,22–26] This implicates that the stability of the grown layers has to be checked carefully every time. In Sec. VII, we will briefly come back on this discrepancy in the observed stability.

Reduced average magnetic moments are often observed[10,19,21] in bcc Co layers grown on GaAs. Values between $1.4\mu_B$ and $1.55\mu_B$ per Co atom are found. Theoretical calculations,[16,27] however, give $1.7\mu_B$ per Co atom. The low measured average moment appears to be caused by a strong interdiffusion at the interfaces over at least several nanometers. The moment at the center of the layers does correspond to the expected value.[21] This interdiffusion may improve the long-range order and diminish the number of defects, thus seeming to stabilize the bcc structure as measured by long-range surface techniques such as low-energy electron diffraction (LEED). It may, however, cause the local physical and magnetic structure to deviate from that of pure bcc Co. Thus, in order to verify the presence of bcc Co, which is both structurally and magnetically pure, not only the structure must be determined, but it also has to be verified that the local magnetic moment has the correct value.

An ideal way to measure both properties at the same time is ^{59}Co NMR, which provides the distribution of Co hyperfine fields, being a direct measure of both the local atomic structures and the local magnetic moments in the entire Co layer. NMR studies of bcc Co grown on Cr(110),[11] Fe(110),[11,22] Au,[12] and τMnAl (Ref. 26), show that in zero applied field, pure bcc Co is characterized by a resonance line at a frequency of 199 MHz, with a full width at half maximum (FWHM) of about 10–15 MHz for well-grown layers. This frequency is about 20–30 MHz lower than the frequencies for the fcc and hcp phases of Co. The width of the bcc Co resonance line is comparable to the fcc and hcp Co linewidths in typical thin films.[8] The lack of a NMR signal at 199 MHz for a measured structure is the direct proof of the absence of both structurally and magnetically pure bcc Co.

Most groups find stability limits of about 1–3 nm.[11,12,22–26] The exact value depends sensitively on the growth method, temperature and speed, and on the specific substrate. The most frequently used substrates, apart from GaAs, are Fe and Cr. Growth by molecular beam epitaxy (MBE) is found to produce the highest stability when the substrate temperature is between room temperature and 200 °C for growth on Fe or between 150 °C and 350 °C for growth on Cr. Lower growth temperatures usually result in a lower long-range quality and higher temperatures induce more interdiffusion. The stability ranges of bcc Co on (001) and (110) surfaces are comparable, but (001) usually shows slightly larger interdiffusion. Extensive NMR measurements on Co/Fe(001) multilayers[22] indicate that interdiffusion in these structures is limited to about 0.6 nm. However, Mössbauer measurements on similarly prepared samples show no significant interdiffusion,[28] hereby demonstrating the strong dependence on preparational details.

The fact that bcc Co is not truly metastable results in a large variation of the observed strains, varying from $c/a = 1.15$ for 2 ML of Co on Ag(001),[29] via several results close to true bcc with $c/a = 1.0$ (Refs. 13 and 25), to values close to the predicted metastable bct phase with $c/a = 0.92$.[30,31] For similar growth on the same substrate different lattice parameters are observed, which means that the exact structure also depends strongly on the experimental details. It is thus not possible to get the precise lattice parameters from the literature. The large variety in strains, however, also creates the possibility to stabilize various phases of strained bcc

Co by choosing substrate and growth conditions. These differently strained phases give a wider choice of materials to be used in device structures.

Very few studies have been performed on the influence of additional layers on the stability of bcc Co (Ref. 22) and none have been reported on the influence of top layers made of a different material other than the substrate. However, for use in a device structure, the growth of extra layers on top of the bcc Co layer is indispensable. The material of these extra layers cannot be freely chosen, but is imposed by the desired functionality. In most reports, characterization is performed before deposition of a top layer. However, due to the low maximum thickness of the bcc layers, the influence of the additional layer may be quite large, especially when made of a non-bcc-inducing material. It is thus better to characterize the covered Co layer than to use only *in situ* characterization during growth.

III. EXPERIMENT

The bcc Co layers were prepared by MBE on Fe(001) buffer layers, grown on either GaAs(001) or on Ge(001) substrates. Growth on Fe was chosen instead of a direct growth on GaAs because of the commonly observed interdiffusion problems. The substrates were cleaned by sputter-anneal treatments until a clear (4×6) reconstruction was observed by LEED for GaAs, or a (2×1)-reconstruction in the case of Ge, and no contamination could be detected by x-ray photoelectron spectroscopy (XPS) and Auger electron spectroscopy (AES). GaAs(001)-(4×6) is a Ga-rich reconstruction, which prevents large-scale interdiffusion of As into and through the Fe layer. The growth of Fe on Ge was initiated at room temperature and continued after a few nanometers at a temperature of 200 °C. This two-step growth is necessary in order to obtain a smooth layer, without Ge diffusing all the way to the top of the layer. The background pressure during growth always stayed below 10^{-10} mbar. On GaAs, Fe was grown at room temperature at a rate of about 1 ML/min. The growth rate was measured by a calibrated quartz-crystal microbalance. The final Fe thicknesses lay between 5 and 15 nm. Subsequently, thin Co layers were deposited at room temperature with varying thicknesses between 0.6 and 4 nm. These layers were covered either with 5.0-nm Fe, with 3.0-nm Cu, or with 2.3-nm Al, which was subsequently plasma oxidized for 200 s to form Al_2O_3.[42]

The growth quality of these layers was checked *in situ* by LEED, scanning tunneling microscopy (STM), XPS, and AES. The physical structure of the Co layers was determined *ex situ* by ^{59}Co NMR. The NMR experiments were performed at 1.5 K in zero applied field.[8,32] NMR measurements provide a way to determine the relative amounts of Co with specific hyperfine fields, corresponding to a distribution of Co atoms over different structural environments (e.g., fcc, hcp, bcc, and structures with neighboring foreign atoms). Among the main advantages of NMR are the possibility to directly observe buried layers, the fact that no long-range order in the layers is necessary, and that the sensitivity is sufficient for measuring single layers with thicknesses well below 1 nm. This high sensitivity is of importance for this study. In contrast to studies with Fe on both sides, it is not possible to grow multilayers of Al_2O_3-capped Co layers, because Al_2O_3 is not a bcc-inducing material. Contrary to usual NMR procedures, the spectra are not corrected for the influence of the rf-pulse power. For the part of the spectrum below about 240 MHz, the correction has a negligible influence. For frequencies above 240 MHz, the correction induces an overestimation of the signal strength, caused by the relatively high noise at higher powers. This strong influence of the noise is created by the low signal strength in this region for a single Co layer. In order to avoid these misrepresentations, the correction has been omitted altogether for all presented spectra. The magnetic properties of the layers were measured by a superconductive quantum interference device (SQUID) and by the magneto-optical Kerr effect (MOKE). Finally, bcc Co was implemented in bcc $Co/Al_2O_3/Co$ tunnel junction structures for measurements on the magnetotransport properties.

IV. GROWTH CHARACTERIZATION

The details of the growth of Fe on GaAs(001) or Ge(001), and of Co on Fe(001) depend strongly on growth parameters as evidenced by the large number of growth results reported in the literature, which are very often at variance with each other. Thus, it is important to always accurately check the crystal quality of the grown layers.

Our first characterization is performed *in situ* by means of LEED. In Figs. 1(a) and 1(b) the LEED patterns of the two different substrates used are presented. The Ge(001) surface is clearly (2×1) reconstructed [Fig. 1(a)], while the GaAs(001) surface shows a (4×6) reconstruction. This reconstruction is probably a mixture of (4×2) and (2×6) reconstructions, both however leading to the same growth of iron, including the same uniaxial anisotropy.[33] Deposition of Fe gives the same results for both substrates, independent of the thickness. The LEED pattern of 5.0-nm Fe on GaAs(001) [Fig. 1(c)], shows sharp spots in the $\langle11\rangle$ directions and quite broad $\langle01\rangle$ direction spots for which the out-of-plane diffraction condition is not perfectly fulfilled. Without roughness this condition would not have been relevant and clear $\langle01\rangle$ spots would have been present. The observed pattern indicates that the Fe grows in the expected (001) bcc structure, but with some roughness. The growth mode found by measuring LEED patterns at different energies indicates the presence of terraces or pyramids in the structure, in agreement with results previously found by Gester.[34]

LEED patterns for 0.85-, 1.35-, and 2.0-nm Co, grown on top of iron, are shown in Figs. 1(d)–1(f), respectively. At least for the two thinnest Co layers the registry of the iron lattice continues in the Co layer. Thus, the Co is also growing in the bcc(001) phase and shows a good order on the LEED coherence length scale. However, the background intensity indicates the presence of quite some roughness. Apart from the $\langle11\rangle$ and $\langle01\rangle$ spots, a $c(2\times2)$ reconstruction is clearly observed, getting stronger for larger thicknesses, as evidenced by the innermost points in the $\langle11\rangle$ directions. As determined by Kim *et al.*,[25] the $c(2\times2)$ reconstruction corresponds to the onset of hcp Co, with a growth in the $(11\bar{2}0)$

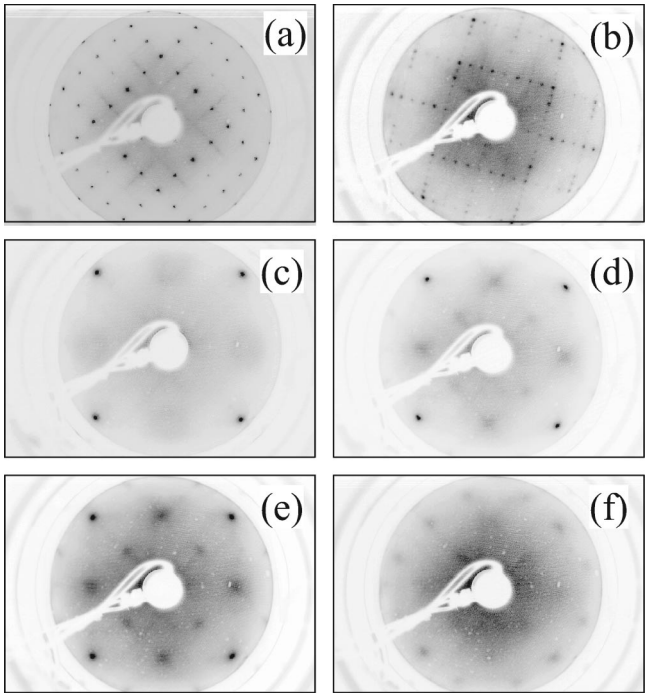

FIG. 1. LEED patterns of bcc Fe and Co on GaAs(001) or Ge(001). The electron energy is about 100 eV, but not exactly equal for all images. Orientation of the samples is also not the same for all images, but about equal for (c)–(f), with the sharp corner points corresponding to the first-order peaks in the ⟨11⟩ directions. Clean Ge(001) (2×1) (a) GaAs(001) (4×6) (b), GaAs(001)/5.0-nm Fe (c), GaAs(001)/5.0-nm Fe/0.85-nm (d), 1.35-nm (e), or 2.0-nm Co (f).

direction. The in-plane structure of this hcp phase fits with some anisotropic compression on the bcc structure by means of a rotation of 45°. In fact, the only difference between this distorted hcp phase and the bcc phase for a single layer lies in the position of the central atom of the hcp structure, which is not centered as it is in the bcc structure and gives rise to the $c(2\times2)$ reconstruction. Thus, it may very well be possible that this structure is an intermediary growth structure of the top of the bcc Co, which may be changed into a true bcc structure by deposition of an extra Co layer. Indeed, we find that the $c(2\times2)$ reconstruction does not immediately give way to the hcp phase upon deposition of extra Co. Structural characterization by NMR, which measures the bulk and not only the surface of the layer, has proven that the $c(2\times2)$ reconstruction does indicate an intermediary growth structure and not an alteration into the hcp phase, as shown further on. For the 2.0-nm-thick Co layer the background has become very strong, indicating a considerable disorder, and the $c(2\times2)$ reconstruction is also relatively strong. However, LEED patterns measured at a lower electron energy (50 eV) still show sharp spots for this thickness. Together with the fact that only a part of the samples grown with this thickness still show discernable LEED patterns, these results point to 2 nm being around the maximum stability thickness for uncovered bcc Co, at least with our growth procedure.

In Fig. 2(a) LEED *I-V* curves of the [00] spot measured at an angle θ of 6° for the pure iron layer and the same three

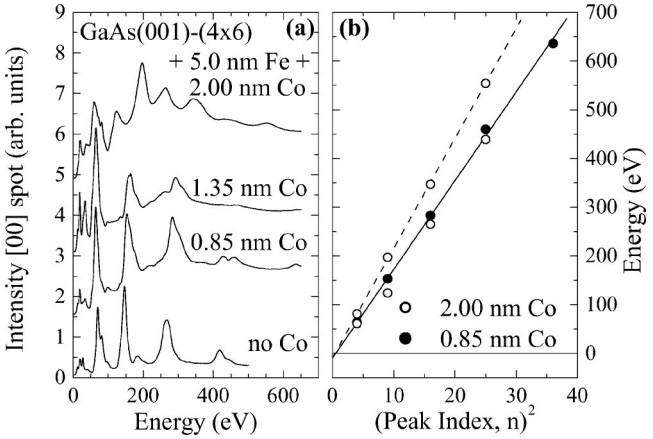

FIG. 2. LEED *I-V* curves (a) and *I-V* peak energy versus peak index squared (b). Curves are shown for 5.0-nm Fe on GaAs(001) and for three different thicknesses of Co on top, showing the small difference in the out-of-plane lattice parameter between Fe and bcc Co and the appearance of a different Co phase at 2.0 nm thickness. For clarity, the curves are shifted on the intensity scale. The peak energies are plotted for two Co thicknesses and show two different slopes (which are proportional to the out-of-plane lattice parameter) for the thickest Co layer.

Co thicknesses shown in Fig. 1 are plotted. The two thinnest Co layers give peaks which are only slightly shifted compared to the Fe buffer layer. The thickest Co layer, however, shows two sets of peaks, one of which roughly corresponds to that of the thinner layers and the Fe substrate. This confirms the phase transition that is occurring at this thickness. A kinematical estimate of the out-of-plane lattice constant is derived from the energies at which the consecutive single-scattering peaks are found, as shown in Fig. 2(b). This procedure is justified for these layers because the absence of strong multiple-scattering features indicates the relative unimportance of these effects. Also, the sharpness of the peaks gives an indication that the influence of relaxation at the surface is not too large. All fits of the peak position versus the peak index squared give an inner-potential shift of about 10 eV, as expected. For the substrates an out-of-plane lattice constant $a=0.564\pm0.002$ nm is found, which is consistent with their bulk lattice constant $a=0.5654$ nm. The iron buffer, however, is found to be expanded 1.5% out of plane compared to the bulk value $a=0.2866$ nm. This expansion does not significantly depend on the thickness or the substrate. The strain in one direction can be related to the strain in perpendicular directions by means of the elastic constants of the material. Bulk elastic constants show that the out-of-plane lattice parameter $c=0.291\pm0.002$ nm corresponds to an in-plane lattice parameter $a=0.281\pm0.002$ nm. This is half of the lattice parameter of the substrate. Thus, Fe does not show significant relaxation for layers up to 15 nm thickness. This corresponds to results found for 1.5-nm-thick Fe grown on GaAs(001)-(4×6) by Gordon *et al.*[35] Other reports show fully relaxed Fe layers of thicknesses above 1.5 nm,[36] but strained iron films with thicknesses up to 160 nm have also been reported.[37]

The out-of-plane lattice parameter of the Co grown on this strained Fe layer is found to be $c=0.287\pm0.002$ nm,

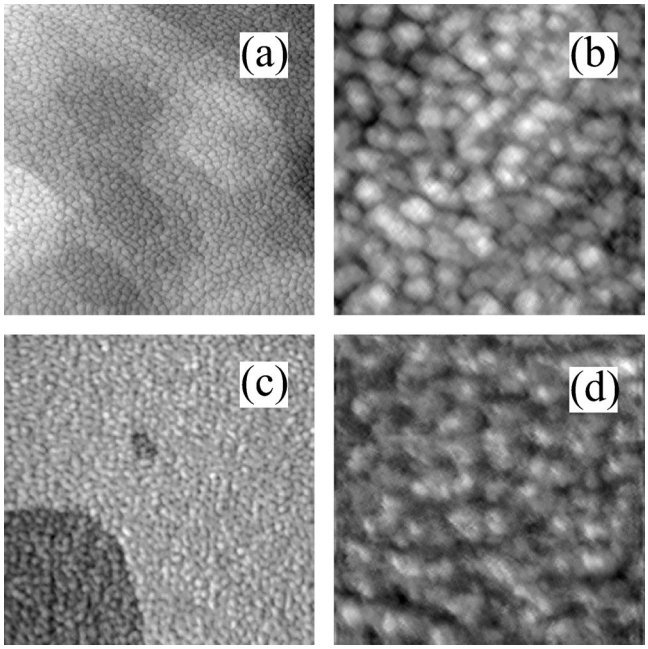

FIG. 3. STM images of 5.0-nm Fe(001) grown on GaAs(001) (a,b) and of 1.5 nm Co grown on an Fe(001) whisker (c,d). The total area of (a) and (c) is 200×200 nm^2 and of (b) and (d) 50×50 nm^2. The height differences on a terrace are about 0.8 nm for the Fe(001) layer and about 0.14 nm for the Co layer. The grainlike features have a typical diameter of about 5 nm for both structures.

which is significantly larger than the unstrained lattice parameter of bcc Co (0.283 nm). This is remarkable because usually an out-of-plane contraction is observed for growth of Co on Fe.[25,31] However, in these studies Co was grown on top of unstrained single-crystalline Fe(001), while in our case there is still a residual strain in the Fe layer, which may have an influence on the growth of the Co layer. In view of the reports of bcc Co with various strains, which strongly depend on the exact substrate and growth conditions (see Sec. II), this value is not unreasonable. For the thickest Co layer shown (2 nm), one of the two observed series of peaks corresponds to a structure that still has the same lattice constant. The other series gives an out-of-plane lattice constant of $c=0.261\pm0.003$ nm. This matches hcp Co oriented in the $[11\bar{2}0]$ direction with about 4% out-of-plane strain, in agreement with earlier results.[31]

The roughness in the Fe and Co layers found by LEED measurements is corroborated by STM measurements, which show granular features with typical lateral sizes around 5 nm. In Fig. 3(a) and 3(b) STM measurements of 5.0-nm Fe grown on top of GaAs(001) are shown. Step edges of the GaAs are still clearly visible. The maximum height differences within one terrace amount to about 0.8 nm, with a root-mean-square roughness of 0.25 nm. The observed structure is comparable to the pyramidal features described by Gester *et al.*[34] showing gradual slopes instead of abrupt steps.

The deposited Co will grow on this relatively rough Fe surface. In order to determine the inherent roughness and growth behavior of bcc Co layers on bcc Fe, these have also been grown on an Fe(001) whisker, because this has perfectly flat terraces. STM measurements on a 1.5-nm-thick Co layer are shown in Figs. 3(c) and 3(d). In the large-scale picture some steps on the Fe(001) whisker are visible. On the small-scale image, the height differences are about 0.14 nm, with a root-mean-square roughness of 0.04 nm. The different 5-nm granular features cannot correspond to grains with different orientations. If that would have been the case no LEED pattern could have been observed, since the correlation length for LEED is larger than the size of these features. Thus, the crystal structures in the different features have to be in registry with each other. There may however be vertical stacking faults separating them. The growth of Co on Fe whiskers seems to be comparable with the growth of Fe on GaAs in physical appearance, showing comparable feature sizes and roughness in STM, if the difference in thickness is taken into account.

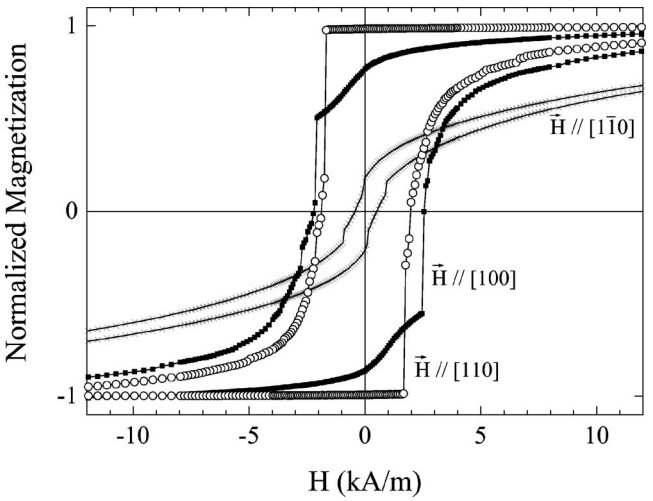

FIG. 4. Magnetization curves of GaAs(001)/5.0-nm Fe/1.2-nm Co/3.0-nm Cu along several axes as measured by SQUID, showing both cubic and uniaxial anisotropies. The curves have been normalized on the saturation magnetization. The measurements have been performed at a temperature of 5 K.

It is known that well-grown Fe layers on GaAs(001)-(4×6) show a combination of a cubic anisotropy and a uniaxial anisotropy caused by the interface.[38,39] In order to check these properties of our layers, magnetization curves have been measured both by SQUID and by MOKE on 5-nm Fe layers grown on GaAs(001), with up to 2-nm Co on top. The magnetization behavior is mainly that of the Fe layers as these are four times thicker than the Co layers. Typical SQUID loops are shown in Fig. 4. As expected, there is a cubic anisotropy inherent in the structure with $\langle100\rangle$ as the easy axes and a uniaxial anisotropy caused by the structure of the GaAs interface, with the easy axis in the [110] direction. The combination of these two anisotropies causes the steps in the magnetization curve for the [100] direction.[38,39] Apart from the size of the magnetic moment, the magnetization behavior of the structures is the same for Fe buffers and Fe buffers with Co layers on top. As usually found, the uniaxial anisotropy is stronger than the cubic one for these thicknesses, resulting in an easy axis along the [110] direc-

tion. The $[1\bar{1}0]$ direction shows a hard axis loop and [100] is intermediary, showing the typical two distinct switching fields found for mixed anisotropies.[40]

V. INFLUENCE OF ADDITIONAL LAYERS

Spin-echo ^{59}Co NMR measurements on buried Co layers were performed as a direct, definitive check on the presence of pure bcc Co in the layers for different additional layers on top of the Co. As a reference and check, some measurements were performed on Co layers which were sandwiched between Fe layers. Since Fe stabilizes the bcc structure in Co, one expects the structure to be left intact and comparable to uncovered bcc Co layers, although, of course, an extra interface is created and some interdiffusion may occur. The results for 1.0- and 2.0-nm-thick single Co layers sandwiched between Fe are given in Fig. 5(a) and are comparable to earlier NMR results on Co/Fe multilayers.[22]

For the 1.0-nm-thick layer a sharp line at $f=199$ MHz is observed (FWHM 9 MHz), comprising about 40% of the Co intensity. No lines are observed at 216, 220, and 228 MHz, apart from the continuous background caused by some interdiffusion at the interfaces. This directly indicates that the bulk part of the Co layer is situated in a chemically, structurally, and magnetically pure bcc phase, thereby directly proving the absence of magnetic or non-magnetic impurities, or other crystal phases. The small bump found at 209 MHz corresponds to Co atoms with 1 Fe nearest neighbor.[22] At the left side of the bulk peak, some intensity centered around 185 MHz is observed, corresponding to about 0.13 nm of Co. This probably corresponds to vertical stacking-faultlike structures in the Co, where the distance between the Co atoms is larger than in the perfect bcc phase. For the 2.0-nm-thick layer, although the highest intensity is still found at 199 MHz, a lot of extra intensity is observed at frequencies corresponding to the fcc and hcp phases and at frequencies in between those phases and the bcc phase. This is a clear sign that at least parts of the Co layer are already transforming to more stable crystal phases. For even thicker layers (not shown) a distinct peak appears at a frequency of about 220 MHz, corresponding to ordered fcc or hcp Co. For these thicknesses the intensity at 199 MHz decreases indicating that a part of the already grown bcc Co transforms to a close-packed structure upon deposition of extra Co.

The position of the bcc peak is influenced by strain in the layer, however as these influences depend on the volume change, strain which is almost volume conserving will not be noticed. In any case, neighboring peaks that are not separated in the spectrum (corresponding, for example, to domain walls) may also cause an apparent shift of the bulk line. The results are in agreement with those found earlier for Co/Fe multilayers[22] with respect to the peak widths and the stability of the bcc Co, although somewhat less interdiffusion at the interfaces is observed in our case.

As shown above and also already demonstrated by other groups, the stability of bcc Co is not negatively influenced by growing an Fe layer on top of the bcc Co layer. To be used in device structures, however, usually Cu (giant magnetoresistance structures) or Al_2O_3 layers (MTJ's) are required on top of the bcc Co. Of these Cu might be expected to have a deteriorating influence on the stability of bcc Co. Since Cu is known to be a good template for growth of the fcc phase of Co,[8] it is quite probable that it has a negative effect on the

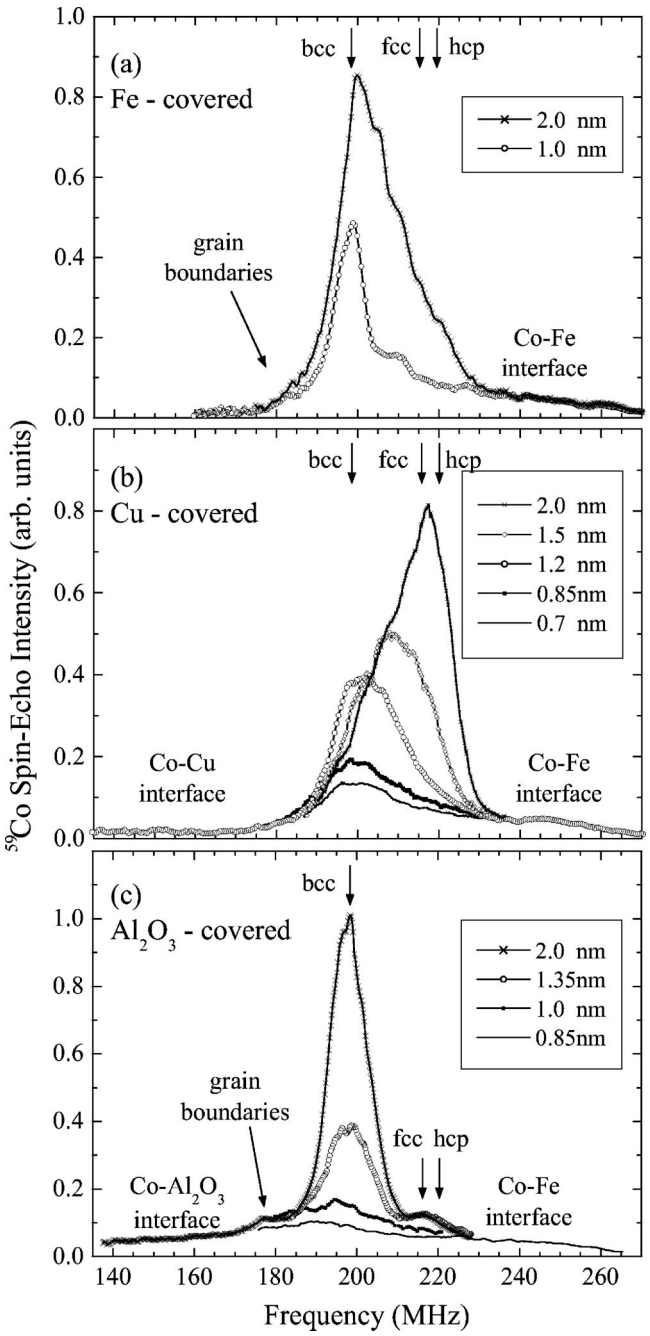

FIG. 5. ^{59}Co NMR spectra of Co layers of various thicknesses grown on Fe(001) and covered with Fe (a), Cu (b), or Al_2O_3 (c), respectively. The measurements have been performed at 1.5 K. The expected positions for the bcc, fcc, and hcp phases are indicated. The small peak at 209 MHz for the Fe-covered layers corresponds to Co with 1 Fe nearest neighbor. The high-frequency tail of the spectrum is virtually independent of the Co thickness. For clarity, this part of the spectrum is only plotted for one thickness. No difference is seen for growth on either Ge(001)/Fe(001) or on GaAs(001)/Fe(001) layers.

stability of the bcc phase, which has a very different lattice parameter. This is indeed seen in Fig. 5(b), where NMR spectra of various thicknesses of Co capped by Cu are plotted. For the lowest thicknesses (up to 1.2 nm), the maximum NMR intensity is still at a position corresponding to bcc Co, but the FWHM of the peak is already increased to 22 MHz. Besides this, the peak shows a clear high-frequency tail up to about 225 MHz. This tail is likely to be caused by Co which is transformed to the more stable fcc or hcp phase. This is confirmed by results for Co layers of 1.5 and 2.0 nm thickness, where the main part of the signal is found to gradually shift towards the equilibrium fcc or hcp frequencies. For the 1.5-nm-thick sample, a broad peak is found at 208 MHz, a resonance frequency with which no ordered Co phase is associated. This simply means that the bcc phase and the fcc/hcp phase of Co are not well-separated phases in this case as they are in the case of Fe capped layers. The crystalline order on an atomic scale is very low, resulting in a kind of random stacking and producing resonance frequencies intermediate to those of bcc and fcc/hcp. For the 2.0-nm-thick Co layer, most of the intensity is already observed at about 220 MHz. Already at 1.5 nm thickness the intensity at 199 MHz is decreasing, implying that less bcc Co is retained and that the bcc phase does indeed transform to other phases. The intensity of the Co-Cu interface is relatively low as compared with the rough surfaces found by STM. This is probably caused by a flattening of the Co layer in the process of recrystallization towards a close-packed structure. Thus in contrast to coverage by Fe layers, Cu coverage recrystallizes the already grown bcc Co, giving a disordered atomic arrangement in between bcc and fcc/hcp. This recrystallization most likely removes the surface roughness of the Co layer.

In Fig. 5(c), the influence of Al_2O_3 top layers, which are very important for use in magnetic tunnel junctions, is shown. The Al oxidation time was chosen in such a way that no oxidized Co or unoxidized Al is observed by XPS. For thicknesses up to 2.0 nm a single peak at 198 MHz is observed with a FWHM of about 11 MHz, comparable to the Fe-capped layers. The intensity around 220 MHz does not grow upon increasing the thickness from 1.35 to 2.0 nm, although there seems to be some intensity which may be associated with a few local defects in the sample. For these layers the maximum stability is about 2.0 nm, since other similar samples did show a transformation around this thickness, just like in the case of Fe capping. For thinner layers a clear peak is not observable, since the spectrum shows interface intensity on both sides of the bulk line. This observation, together with the intensity from grain-boundarylike structures around 180 MHz, causes an apparent shift of the bulk frequency from 199 MHz to about 190 MHz for thinner layers. The intensity of the Co-Al_2O_3 interface corresponds to about 3 ML of Co with at least one non-Co nearest neighbor. This is caused by the roughness of the top of the Co layer, which is not reduced in this case and probably also by the diffusion of some Al into the vertical stacking faults which exist in the Co layer. The exact structure of the Co/Al_2O_3 interface itself cannot be determined, since it is an interface with an amorphous material, which does not give well-defined local environments for the interface Co atoms.

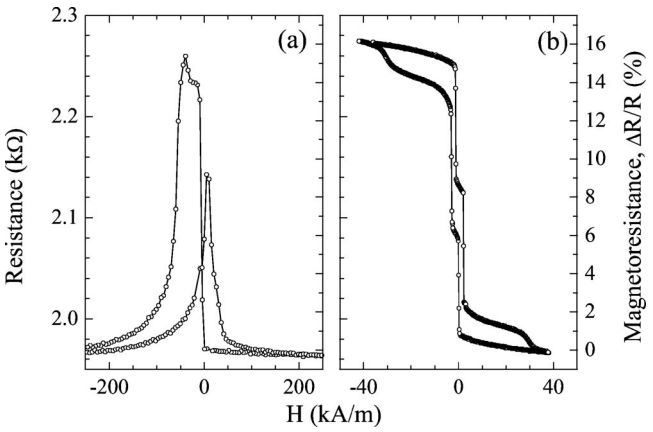

FIG. 6. Magnetoresistance measurement of a 0.8-nm (bcc Co)/Al_2O_3/Co/CoO_x junction at 10 K. The observed tunnel magnetoresistance is 16.4%. The field is applied along the [100] direction of the bcc Co. A full scan, which destroys the exchange bias after the first sweep by a training effect of CoO_x, is shown in panel (a). A minor loop, in which the magnetization of the top Co layer is kept in the equilibrium direction caused by the exchange bias, is shown in panel (b).

These results show that bcc Co can be used in device structures for thicknesses up to 2.0 nm, when it is capped with Al_2O_3. However, devices using a Cu layer on top of the Co layer, will at best have a mixed crystal phase, with non-bcc Co at the top of the structure near the Co-Cu interface. The first result is particularly useful for magnetic tunnel junctions, since tunneling from a bcc(001) Co bottom electrode is feasible. Tunneling is particularly sensitive to the top interface of the Co layer,[41] but, although there is quite some interface roughness, the local structure is still bcc. Further, as demonstrated, the roughness is not extensive enough to prevent the formation of a good MTJ. For layers of about 1-nm Co, the Co is single crystalline with a (001) orientation of the entire layer, thus giving the possibility to use this structure as a single-crystal bottom electrode.

VI. MAGNETIC TUNNEL JUNCTIONS

Now that the stability of bcc Co against coverage with Al_2O_3 has been established, we can try to create magnetic tunnel junctions with single-crystal bcc(001) Co bottom electrodes. We used the growth procedures given above for creating suitable bcc Co layers of about 1.0 nm thickness. GaAs(001)/5.0-nm Fe was always used as a substrate. As a top electrode, Co is deposited on the Al_2O_3 barrier. In order to make both a parallel and an antiparallel alignment of the electrodes possible, the top Co layer was partly oxidized after deposition, so that an antiferromagnetic CoO_x layer was obtained, which causes exchange biasing of the top layer. The junction area is $300\times300\ \mu m^2$. Details of the growth procedure are given by LeClair *et al.*[42]

The resistance of a 0.8-nm (bcc Co)/2.3-nm Al_2O_3/15-nm Co/CoO_x junction at 10 K versus the applied magnetic field is shown in Fig. 6. A full loop, starting at high positive fields, is plotted in Fig. 6(a). It shows both a parallel and an almost antiparallel alignment of the electrode magnetization and a

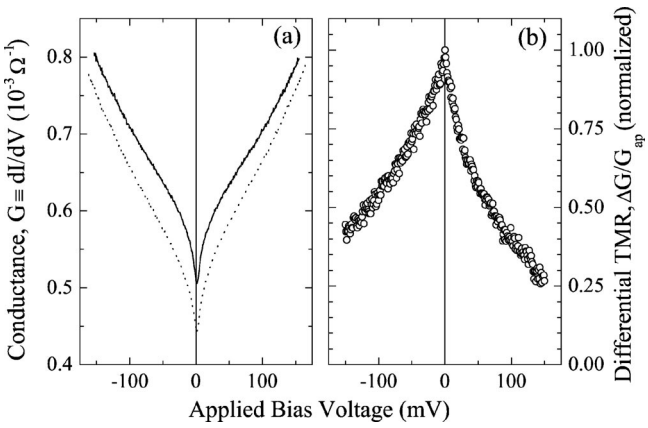

FIG. 7. Conductance versus bias voltage at 10 K (a). The parabolic signature of free-electron tunneling is clearly present together with a low-voltage magnon characteristic. In (b), the decay of the differential TMR with applied bias voltage is shown. Note that the voltage dependence of the TMR ($\Delta R/R_p$) differs from that of the differential TMR ($\Delta G/G_{ap}$). The differential TMR becomes negative for higher bias voltages, while the TMR always stays positive.

magnetoresistance of roughly 16%. The return sweep of the field does not show a fully antiparallel alignment due to a training effect in the CoO_x.[43] However, by measuring minor loops and not switching the top Co layer away from the direction imposed by the CoO_x, magnetoresistance measurements can be performed at repeated field cycles. This is shown in Fig. 6(b). The steps around zero field are caused by the uniaxial anisotropy of the Fe bottom layer, which is always aligned parallel with the bcc Co bottom electrode. The changes in resistance at about ± 30 kA/m are probably caused by small rotations of the top Co magnetization. For temperatures close to room temperature the exchange biasing is not ideal any more, giving nonperfect alignment of the magnetization directions. At this moment it is not clear whether the relatively low value of the magnetoresistance is an intrinsic property of bcc(001) Co, as in some other epitaxial systems,[6] or because the growth of these preliminary bcc Co junctions is not yet fully optimized.

Typical conductance (dI/dV) versus bias voltage curves are given in Fig. 7(a). The conductance curves can be described by a parabolic contribution from regular elastic tunneling[44] and a linear contribution from magnon-assisted tunneling at low bias.[45] In Fig. 7(b), the normalized, differential tunnel magnetoresistance (TMR) is plotted as a function of bias voltage, showing the typical behavior of a tunnel junction structure.[46] The top electrode consists of polycrystalline fcc and hcp Co, which has a different electronic structure than the bcc Co(001). This causes a difference in bias dependence between tunneling from top to bottom electrode and tunneling from bottom to top electrode. This difference is seen as an asymmetry, as observed in the differential tunnel magnetoresistance.[7] Further optimization and more systematic studies of these junctions may be necessary to further exclude roughness and exchange bias related problems.

These magnetoresistance measurements show that the slight roughness of the bcc Co layer is not an obstacle to the formation of a good MTJ. Bcc Co can indeed be used as a bottom electrode material and a tunnel magnetoresistance of about 16% is obtained at low temperatures.

VII. DISCUSSION

The stability of the bcc Co layers of about 2 nm found in our experiment fall in the range commonly observed by different groups on a variety of substrates.[11,12,22–26] The fact that thicker layers were not obtainable agrees well with the theoretical prediction that bcc Co is not metastable, but strain induced.[16] We also tried to grow bcc Co directly on GaAs(001) instead of on an Fe buffer layer. Also on these substrates we were not able to reproduce the layers of more than 10 nm thick reported by Bland *et al.*[21] The stability limits in the study by Bland *et al.*, together with those in studies by Prinz *et al.*,[10,19,20] where thicknesses larger than 30 nm were obtained on GaAs(110), deviate strongly from those observed by almost all other groups. It would be a very important advantage for the fabrication of bcc Co if these thicknesses could be reproducibly obtained. What causes the difference in stability ranges is not quite clear. NMR measurements on 2-nm-Co layers grown on GaAs(001), with the growth parameters as described by Prinz *et al.*,[10] either show that the major part of the Co is nonmagnetic due to interdiffusion or that the Co is in the fcc or the hcp phase.

Despite the extensive reported structural analysis on the thick bcc layers, the reason why the stability limit is so high for these bcc structures is still unclear. It may be that As acts as a surfactant, floating on top of the Co, thereby stabilizing the bcc structure. A similar effect has been observed from an oxygen surfactant,[25] this effect, however, only stabilized the bcc Co up to 3 nm thickness. On the other hand, it is also possible that the thick layers are stabilized by impurities (mainly As), diffusing into the Co. The presence of significant interdiffusion of As and Ga into these layers was already shown directly,[47] but the amounts far away from the interfaces were found to be very low ($<3\%$). However, the low average magnetic moment observed, of $1.4\mu_B$–$1.55\mu_B$ per Co atom,[10,19,21] seems to indicate that interdiffusion may go further than expected. Impurity stabilization might also explain the fact that the 35.7-nm-thick bcc layer was never reproduced by Prinz *et al.* and that this layer was grown at a higher growth rate and less well-controlled conditions than other attempts.[16]

All characterization results on the thick layers do show that the structure consists of a good quality bcc phase. However the effect of low, stabilizing, impurity concentrations is hard to determine. NMR might give a definitive answer to the question whether these layers consist of both structurally and magnetically pure bcc Co (see Sec. II). The only reports of NMR measurements on these layers[19,21] show NMR spectra with a maximum intensity around 167–170 MHz. These values agree with the reduced average magnetic moment of $1.4\mu_B$–$1.55\mu_B$ per Co atom in these layers. They do not, however, correspond to the bcc Co resonance line at 199 MHz. In both cases no significant NMR signal is observed at this frequency, which would directly seem to indicate that quite large amount of impurities is located throughout the layer, thereby stabilizing the bcc structure but disturbing the

bcc Co properties. Further NMR measurements on the bcc Co layers on GaAs by Prinz *et al.* and Bland *et al.* may give an answer to this question.

The layers grown in this study have been shown by NMR to consist of pure bcc Co. Since bcc Co is strain induced, there may be some difficulties on the stability of the layer in time, which would be detriment to its usefulness. We checked this by repeating the NMR measurements on our samples, two years after growth and found that none of the samples with Al_2O_3 on top showed any change. The bcc structure was perfectly preserved. Also, annealing for half an hour at 150 °C or 200 °C caused no changes. After two years, the Cu-covered layers also still showed their original structure, but the Co had become magnetically much harder, which is probably caused by oxygen diffusing into the edges of the layer and into the vertical grain-boundarylike structures present. Thus, the bcc structure in layers up to 2 nm is shown to be stable over a period of years.

VIII. CONCLUSIONS

In conclusion, we have established that ^{59}Co nuclear magnetic resonance is an ideal technique for a direct determination of the presence of structurally and magnetically pure bcc Co. We have employed this technique to determine the influence of additional layers on the stability of bcc Co. This is very important for the use of bcc Co in device structures.

After an analysis of uncovered Co layers grown on Fe(001)/GaAs(001) and Fe(001)/Ge(001), which proved them to be bcc up to about 2.0 nm, the Co layers were covered by Fe, Cu, or Al_2O_3. Results for Fe-topped layers are in agreement with those found in the literature for Co-Fe multilayers[22] and show no negative influence on the stability range of the bcc Co. On the other hand, a coverage with Cu, a material which is often used in giant magnetoresistance devices, showed a gradual shift from the bcc phase to the fcc or the hcp phase via a range of intermediate phases. This corresponds to a large-scale transformation of the bcc Co on top of the layer into a locally disordered structure for any Co thickness. Growth of Al_2O_3 on top of Co, which is necessary for application in tunnel magnetoresistance structures, did not show any transformation and left the bcc Co layers intact up to 2.0 nm. The relatively large amount of Co-Al_2O_3 interface signal indicates a rough interface and probably some interdiffusion into grain-boundarylike structures in Co, however, without modifying the bcc(001) structure. The bcc structure was found to be stable over a period of years when covered by Al_2O_3. These results imply that junctions using bcc(001) Co as a bottom electrode can be grown and used to study the influence of the electrode structure on tunneling properties. Junctions using a bcc(001) Co bottom electrode, show, although suffering from some roughness related and exchange bias problems, a magnetoresistance of 16.4% at low temperature.

ACKNOWLEDGMENTS

The work of P.LC. and K.H. was financially supported by the Dutch Technology Foundation (STW).

*Electronic address: h.wieldraaijer@tue.nl

[1] J.S. Moodera, L.R. Kinder, T.M. Wong, and R. Meservey, Phys. Rev. Lett. **74**, 3273 (1995).
[2] J.A. Appelbaum and W.F. Brinkman, Phys. Rev. **186**, 464 (1969).
[3] S. Zhang and P.M. Levy, Eur. Phys. J. B **10**, 599 (1999).
[4] I.I. Oleinik, E.Y. Tsymbal, and D.G. Pettifor, Phys. Rev. B **62**, 3952 (2000).
[5] S. Yuasa, T. Sato, E. Tamura, Y. Suzuki, H. Yamamori, K. Ando, and T. Katayama, Europhys. Lett. **52**, 344 (2000).
[6] S. Yuasa, T. Nagahama, and Y. Suzuki, Science **297**, 234 (2002).
[7] P. LeClair, J.T. Kohlhepp, C.H. van de Vin, H. Wieldraaijer, H.J.M. Swagten, W.J.M. de Jonge, A.H. Davis, J.M. MacLaren, J.S. Moodera, and R. Jansen, Phys. Rev. Lett. **88**, 107201 (2002).
[8] P.C. Riedi, T. Thomson, and G.J. Tomka, in *Handbook of Magnetic Materials*, edited by K.H.J. Buschow (Elsevier, Amsterdam, 1999), Vol. 12 pp. 97–258.
[9] H. Wieldraaijer, P. LeClair, J.T. Kohlhepp, H.J.M. Swagten, and W.J.M. de Jonge, IEEE Trans. Magn. **38**, 2727 (2002).
[10] G.A. Prinz, Phys. Rev. Lett. **54**, 1051 (1985).
[11] P. Houdy, P. Boher, F. Giron, F. Pierre, C. Chappert, P. Beauvillain, K.L. Dang, P. Veillet, and E. Velu, J. Appl. Phys. **69**, 5667 (1991).
[12] J. Korecki, M. Kubik, T. Slezak, M. Augustniak, N. Spiridis, E. Jedryka, M. Wojcik, and S. Nadolski (unpublished).
[13] S.K. Kim, F. Jona, and P.M. Marcus, Phys. Rev. B **51**, 5412 (1995).
[14] P. Wetzel, P. Bertoncini, D. Berling, A. Mehdaoui, B. Loegel, D. Bolmont, G. Gewinner, C. Ulhaq-Bouillet, and V. Pierron-Bohnes, Surf. Sci. **499**, 210 (2002).
[15] W.S. Lew, A. Samad, S.P. Li, L. Lopes-Diaz, G.X. Cheng, and J.A.C. Bland, J. Appl. Phys. **87**, 5947 (2000).
[16] A.Y. Liu and D.J. Singh, J. Appl. Phys. **73**, 6189 (1993).
[17] P. Alippi, P.M. Marcus, and M. Scheffler, Phys. Rev. Lett. **78**, 3892 (1997).
[18] S. Fox and H.J.F. Jansen, Phys. Rev. B **60**, 4397 (1999).
[19] P.C. Riedi, T. Dumelow, M. Rubinstein, G.A. Prinz, and S.B. Qadri, Phys. Rev. B **36**, 4595 (1987).
[20] M.A. Mangan, G. Spanos, T. Ambrose, and G.A. Prinz, Appl. Phys. Lett. **75**, 346 (1999).
[21] J.A.C. Bland, R.D. Bateson, P.C. Riedi, R.G. Graham, H.J. Lauter, J. Penfold, and C. Shackleton, J. Appl. Phys. **69**, 4989 (1991).
[22] J.P. Jay, E. Jêdryka, M. Wójcik, J. Dekoster, G. Langouche, and P. Panissod, Z. Phys. B: Condens. Matter **101**, 329 (1996).
[23] S.J. Blundell, M. Gester, J.A.C. Bland, C. Daboo, E.G.M.J. Baird, and A.J.R. Ives, J. Appl. Phys. **73**, 5948 (1993).
[24] Y.Z. Wu, H.F. Ding, C. Jing, D. Wu, G.L. Liu, V. Gordon, G.S. Dong, X.F. Jin, S. Zhu, and K. Sun, Phys. Rev. B **57**, 11 935 (1998).
[25] S.K. Kim, C. Petersen, F. Jona, and P.M. Marcus, Phys. Rev. B **54**, 2184 (1996).
[26] G. Bruynseraede, G. Lauhoff, J.A.C. Bland, G. Strijkers, J.D. Boeck, and G. Borghs, IEEE Trans. Magn. **34**, 861 (1998).

[27] D.J. Singh, Phys. Rev. B **45**, 2258 (1992).
[28] B. Kalska, P. Blomquist, L. Häggström, and R. Wäppling, J. Phys.: Condens. Matter **13**, 2963 (2001).
[29] H. Li and B.P. Tonner, Phys. Rev. B **40**, 10 241 (1989).
[30] J.D. Boeck, W.V. Roy, C. Bruynseraede, A.V. Esch, H. Bender, C.V. Hoof, and G. Borghs, Phys. Scr., T **T66**, 183 (1996).
[31] G.C. Gazzadi and S. Valeri, Europhys. Lett. **45**, 501 (1999).
[32] W.J.M. de Jonge, H.A.M. de Gronckel, and K. Kopinga, in *Ultrathin Magnetic Structures II*, edited by B. Heinrich and J.A.C. Bland (Springer-Verlag, Berlin, 1994), pp. 279–290.
[33] R. Moosbühler, F. Bensch, M. Dumm, and G. Bayreuther, J. Appl. Phys. **91**, 8757 (2002).
[34] M. Gester, C. Daboo, S.J. Gray, and J.A.C. Bland, J. Magn. Magn. Mater. **165**, 242 (1997).
[35] R.A. Gordon, E.D. Crozier, D.-T. Jiang, T.L. Monchesky, and B. Heinrich, Phys. Rev. B **62**, 2151 (2000).
[36] M. Doi, B.R. Cuenya, W. Keuen, T. Schmitte, A. Nefedov, H. Zabel, D. Spoddig, R. Meckenstock, and J. Pelzl, J. Magn. Magn. Mater. **240**, 407 (2002).
[37] H.-P. Schönherr, R. Nötzel, W. Ma, and K.H. Ploog, J. Appl. Phys. **90**, 1222 (2001).
[38] M. Zölfl, M. Brockmann, M. Köhler, S. Kreuzer, T. Schweinböck, S. Miethaner, F. Bensch, and G. Bayreuther, J. Magn. Magn. Mater. **175**, 16 (1997).
[39] M. Brockmann, M. Zölfl, S. Miethaner, and G. Bayreuther, J. Magn. Magn. Mater. **198-199**, 384 (1999).
[40] F. Gustavsson, E. Nordström, V.H. Etgens, M. Eddrief, E. Sjöstedt, R. Wäppling, and J.-M. George, Phys. Rev. B **66**, 024405 (2002).
[41] P. LeClair, J.T. Kohlhepp, H.J.M. Swagten, and W.J.M. de Jonge, Phys. Rev. Lett. **86**, 1066 (2001).
[42] P. LeClair, H.J.M. Swagten, J.T. Kohlhepp, R.J.M. van de Veerdonk, and W.J.M. de Jonge, Phys. Rev. Lett. **84**, 2933 (2000).
[43] J. Nogués and I.K. Schuller, J. Magn. Magn. Mater. **192**, 203 (1999).
[44] E.L. Wolf, *Principles of Electron Tunneling Spectroscopy* (Oxford University Press, London, 1985), Chap. 8.
[45] S. Zhang, P.M. Levy, A.C. Marley, and S.S.P. Parkin, Phys. Rev. Lett. **79**, 3744 (1997).
[46] P. LeClair, H.J.M. Swagten, J.T. Kohlhepp, and W.J.M. de Jonge, Appl. Phys. Lett. **76**, 3783 (2000).
[47] F. Xu, J.J. Joyce, M.W. Ruckman, H.-W. Chen, F. Boscherini, D.M. Hill, S.A. Chambers, and J.H. Weaver, Phys. Rev. B **35**, 2375 (1987).